BNL-113412-2017-JA

Characterization of TimepixCam, a fast imager for the time-stamping of optical photons

Andrei Nomerotski, I. Chakaberia, M. Fisher-Levine, Z. Janoska, P. Takacs and T. Tsang

Submitted to Journal of Instrumentation

January 2017

Physics Department

Brookhaven National Laboratory

U.S. Department of Energy
USDOE Office of Science (SC),
High Energy Physics (HEP) (SC-25)

Notice: This manuscript has been authored by employees of Brookhaven Science Associates, LLC under Contract No. DE-SC0012704 with the U.S. Department of Energy. The publisher by accepting the manuscript for publication acknowledges that the United States Government retains a non-exclusive, paid-up, irrevocable, world-wide license to publish or reproduce the published form of this manuscript, or allow others to do so, for United States Government purposes.

DISCLAIMER

This report was prepared as an account of work sponsored by an agency of the United States Government. Neither the United States Government nor any agency thereof, nor any of their employees, nor any of their contractors, subcontractors, or their employees, makes any warranty, express or implied, or assumes any legal liability or responsibility for the accuracy, completeness, or any third party's use or the results of such use of any information, apparatus, product, or process disclosed, or represents that its use would not infringe privately owned rights. Reference herein to any specific commercial product, process, or service by trade name, trademark, manufacturer, or otherwise, does not necessarily constitute or imply its endorsement, recommendation, or favoring by the United States Government or any agency thereof or its contractors or subcontractors. The views and opinions of authors expressed herein do not necessarily state or reflect those of the United States Government or any agency thereof.

18TH INTERNATIONAL WORKSHOP ON RADIATION IMAGING DETECTORS
3–7 JULY 2016,
BARCELONA, SPAIN

Characterization of TimepixCam, a fast imager for the time-stamping of optical photons

Andrei Nomerotski,[a,1] **I. Chakaberia,**[a] **M. Fisher-Levine,**[a] **Z. Janoska,**[b,c] **P. Takacs**[a] **and T. Tsang**[a]

[a] *Brookhaven National Laboratory, Upton, NY 11973, U.S.A.*

[b] *Faculty of Nuclear Sciences and Physical Engineering, Czech Technical University in Prague, Brehova 7, 11519 Prague, Czech Republic*

[c] *Faculty of Electrical Engineering, Czech Technical University in Prague, Technicka 2, 16627 Prague, Czech Republic*

E-mail: anomerotski@bnl.gov

ABSTRACT: We describe the characterization of TimepixCam, a novel camera used to time-stamp optical photons. The camera employs a specialized silicon sensor with a thin entrance window, read out by a Timepix ASIC. TimepixCam is able to record and time-stamp light flashes exceeding 1,000 photons with 15 ns time resolution. Specially produced photodiodes were used to evaluate the quantum efficiency, which was determined to be higher than 90% in the wavelength range of 430–900 nm. The quantum efficiency, sensitivity and ion detection efficiency were compared for a variety of sensors with different surface treatments. Sensors with the thinnest window, 50 nm, had the best performance.

KEYWORDS: Photon detectors for UV, visible and IR photons (solid-state); Pixelated detectors and associated VLSI electronics; Timing detectors

[1] Corresponding author.

Contents

1 Introduction

The imaging of fast processes with nanosecond-scale timing resolution is becoming a necessity in many applications such as imaging mass spectrometry, velocity mapping ion imaging, coincidence and covariance imaging, neutron time-of-flight imaging and others, see examples in [1–7]. This manuscript describes the concept of the counting and time-stamping of optical photons, and presents recent results on the characterization of TimepixCam, a fast optical imager [8], which can be used for this purpose. Detection of individual photons and other particles is ultimately a route to capture all available information for the process in which they were produced. Photon counting is already a widely used modality in X-ray imaging [9], where the signal is sufficiently large to detect individual photons directly, and to enable measurement of the time and energy for each of them. High rate capabilities of the associated readout electronics allow fast accumulation of statistics so this information can be efficiently used for imaging.

Ever improving technology is pushing down the energy threshold whilst simultaneously improving the time resolution. Ultimately, this will result in the ability to use the photon counting technique for individual optical photons with an efficiency close to 100%, but we are not there yet. If the goal is to achieve the fastest possible performance, then the current state of the art (in hybrid pixel detectors) for the energy threshold is about 500 electrons, determined by the noise of the front-end electronics, and obtains a time resolution of about 1 ns. While the X-ray photons produce 1000's of charge carriers in silicon depending on their energy (3.6 eV/pair), a single optical photon will typically yield a single electron-hole pair. Therefore, a flash of 1000's of simultaneously emitted optical photons is required to produce a similar signal and achieve the performance outlined above using contemporary electronics.

2 Sensors and test structures

TimepixCam is an optical imager with time-stamping described in more detail in [8]. The main components of the camera are a specialized sensor bump-bonded to the Timepix chip [10], all integrated in the X-Ray Imatek UNO camera with a lens to project images on to the sensor. Figure 1a shows a photograph of the sensor on a daughter board in the camera.

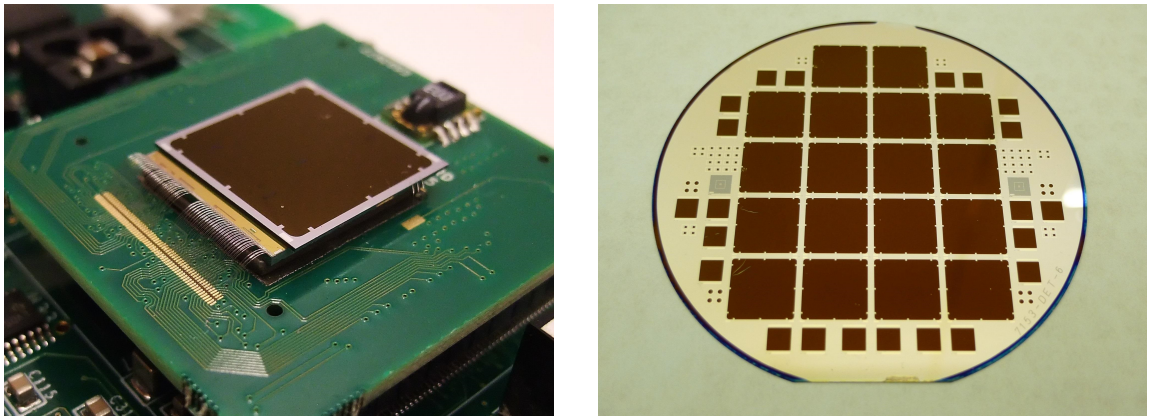

Figure 1. (a) Photograph of the thin window sensor bump bonded to Timepix on a daughter board in the X-Ray Imatek UNO readout, and (b) a photograph of TimpixCam sensor wafer with 18 sensors and various test structures. $5 \times 5\text{mm}^2$ test structures were used for the measurements of quantum efficiency described in the text.

The sensor design considerations have been described in detail in [8]. The thin entrance window of the sensor is the most important feature, as it allows efficient transmission of optical photons to the sensitive volume of depleted silicon. Standard p-on-n 300 μm thick silicon wafers were used for the sensors produced at CNM.

A photograph of the wafer is shown in figure 1b. A variety of test structures were accommodated on the periphery of the wafer to verify the design options and for quality assurance during production. The structures used for the measurements described below were the standard 5mm x 5mm photodiodes, also visible in the figure. After dicing of the wafer, the individual photodiodes were mounted and wire bonded on to simple boards to allow direct measurement of the current and capacitance as a function of the bias voltage. These parameters are not easily measured on the full sensor.

The typical depletion voltage was determined to be about 25V through a standard measurement of the photodiode capacitance. The sensors were typically biased to a higher voltage, 80V, to ensure full depletion of the surface, which is important for good sensitivity, especially at shorter wavelengths. The sensor itself is able to withstand much higher voltages, up to 500V, since it employs a radiation hard design developed for particle physics applications. The photodiode's dark current was measured as a function of the applied voltage up to 100V and typically did not exceed 10's of nA, including the current flowing through the internal guard ring.

A single layer anti-reflective coating (ARC) was applied to the sensors to improve the sensitivity. The ARC was optimized for 430 nm, corresponding to the wavelength at which maximum emission power occurs in P47, a fast phosphor frequently used for these applications. Below, we describe

measurements of the quantum efficiency and sensitivity of the sensors, as well as the efficiency of the camera when used with different sensors. However, before that, it is useful to define exactly what is meant by these terms.

3 Useful definitions

The comparison of different sensors in the camera provides essential information for the sensor design optimization. However, even measurements of the relative performance is far from straightforward given the complexity of the signal processing at the pixel level in the Timepix chip, and also due to the fact that each sensor is attached to a physically different chip. It is therefore important to define what is meant by the terms used when measuring the performance.

Quantum efficiency (QE): the probability that a photon of a given wavelength, which is incident upon a pixel, will be converted into a photoelectron, which will then contribute to the signal in the analog front-end. In practice, the QE is almost impossible to measure directly on TimepixCam due to the imprecise knowledge of the threshold level in electrons, the threshold dispersion across the pixels, and the binary nature of the readout. To perform the measurement we produced photodiodes from the same material, in the same process, and measured their QE directly, as will be explained below.

Sensitivity: the probability that a photon emitted from a specific phosphor or scintillator screen will convert in the detector to produce a photoelectron, and which therefore implicitly includes a geometric factor from the camera's optical system. It is therefore the sensor quantum efficiency convoluted with the output spectrum from a particular screen and lens combination. Sensitivity is an excellent parameter for making like-for-like comparisons of sensor performance, but for the same reasons as stated above, is hard to measure directly.

Camera efficiency: the probability that an ion or photon producing an avalanche on the micro-channel plate (MCP) will be detected by one or more pixels in the camera. In these experiments, the MCP serves as the primary ion or electron detector, and the light flashes are produced by the P47 phosphor placed behind the MCP. This efficiency is the real figure of merit for the performance in a particular experiment. Though directly measurable with the camera, it is a subtle property, with different threshold effects contributing to it. Efficiency does not directly correlate to sensitivity because photons can be 'lost' when they hit a pixel in insufficient numbers to cause the pixel to trigger and latch a timecode, a threshold effect from the binary nature of these time-stamping detectors. A small increase in the gain in the MCP can quickly change the efficiency for a given setup from 0 to 1, even though most of the photons were not being lost in the traditional sense, e.g. due to poor QE.

Bad focusing can compound this 'lost photon' effect; for a poor focus, an MCP signal which yielded enough photons to trigger a pixel may be spread out over a few, causing the efficiency to drop very quickly, despite the sensor having good intrinsic sensitivity.

4 Quantum efficiency

The quantum efficiency is a critical parameter for any sensor used for photon detection. It is defined as the ratio of the number of photoelectrons produced by photons impinging on the sensor, to the total number of the photons, and is usually given as a function of the wavelength. The photocurrent in the sensor can easily be used to measure the nominator in this ratio. However, the estimation of the denominator, the number of incident photons, requires accurate measurement using absolutely calibrated instruments.

Figure 2 schematically shows the experimental setup used for QE measurements of the produced test structures. A laser-driven light source, Energetiq EQ99XFC, emitted a broadband, VUV to NIR uniform CW (continuous wave) with a white spectrum. A one-meter long 200 μm fiber coupled the source to a compact monochromator, Edmund Optics DMC1-01 (DMC1-05 for the NIR light), to allow the wavelength selection in the 350–1100 nm range. The spectral resolution of the monochromator is 4.5 nm FWHM in the visible range and 18 nm in the NIR. The wavelength can be adjusted in steps of 10 to 50 nm, depending on the region of spectral interest. The light after the monochromator was divided into two halves by employing a 2-meter long 200 μm 50/50 fiber splitter. After the splitter, each arm was fed through the same fiber collimators (visible or NIR) before illuminating, correspondingly, the Device Under Test (DUT) and the 918-UV power head of a NIST calibrated Newport 1930C power meter, at normal incidence angle. All wavelengths used for the measurement were verified independently by coupling one arm to a fiber-coupled spectrometer, Ocean Optics QE65000. The DUT was reverse biased at 80 V and the corresponding photocurrent was measured with the Keithley 6485 picoammeter. The DUT, optical power head, and the 50/50 splitter were all housed in a dark box, and the dark photocurrents were measured and subtracted for each wavelength. To completely account for the systematic uncertainty of the measurement, such as imperfect optical power splitting and the wavelength dependence of the 50/50 coupler, the outputs of the splitter were swapped between DUT and the power head, and the measurements were averaged over the two configurations. All measurements were repeated on different days to check the consistency, with good results. Overall, we estimate the systematic uncertainty for the above QE measurements to be less than 5%.

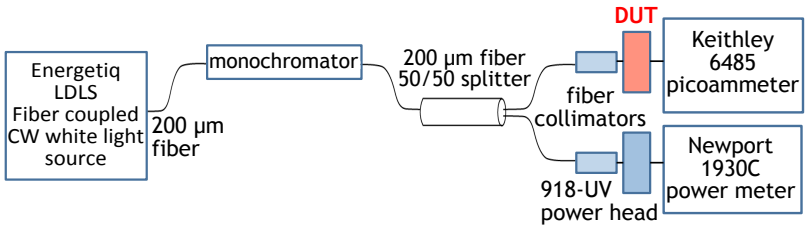

Figure 2. Experimental setup used for the measurements of quantum efficiency of the test structures, see the text.

Figure 3a shows the QE curves for four of the sensors produced, two with ARC and two without, as a function of wavelength. The two sensors without ARC have considerably lower QE, about 70% or below, while the sensors with ARC have QE above 90% for most of the wavelength range. As expected, the thickness of the window passivation affects the QE behavior for shorter wavelengths. The thinnest passivation, 50 nm with ARC, has the highest blue sensitivity. The

quantum efficiency quickly deteriorates with increased thickness of the passivation layer. The other curves shown in the plot correspond to the passivation thicknesses of 120 nm (with and without ARC) and 200 nm. Note that this should considerably affect the sensor sensitivity as defined above, which convolutes QE with the emission spectrum. Two fast screen materials commonly used for this purpose, P47 phosphor and Exalite-404 scintillator, have their spectral maxima at 430 and 405 nm respectively [11]. The QE roll-off at the longer wavelengths is due to the increased transparency of the silicon to the infrared photons. Since the sensors are quite thick, 300 μm, the roll-off starts late, at around 950 nm.

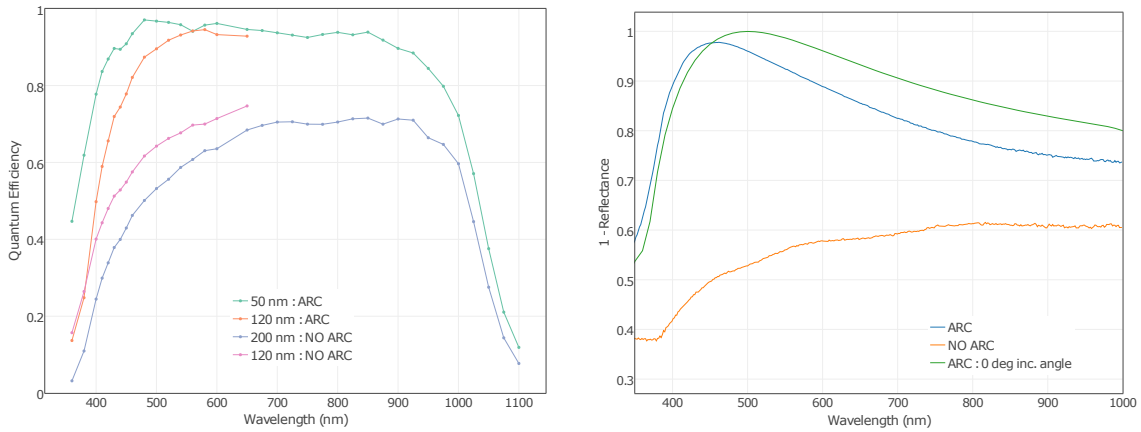

Figure 3. (a) Measured quantum efficiency of the photodiodes as a function of wavelength, and b) the measured (1 - Reflectance) of the photodiodes as a function of wavelength with and without ARC at 45 degrees incidence angle; and a calculated (1 - Reflectance) at zero degrees.

Quantum efficiency can also be evaluated from the reflectance for wavelengths in the range 500–800 nm, where the photon absorption length is small enough that all light is absorbed in the silicon, but is not so small that the surface dead layer has a significant effect, as it does at shorter wavelengths. In this region QE = 1 - R, where R is the reflectance of the sensor.

The measurements were performed using a spectroscopic ellipsometer J.A.Woollam M2000D, which allows measurement of the reflectance for the incidence angles from 45 to 72 degrees (normal incidence is zero degrees) for parallel and perpendicular light polarization. In the following, natural polarization is assumed, which was estimated as the average of the parallel and perpendicular polarizations. The surface reflectance of two photodiodes with 50 nm passivation, with and without ARC, has been measured. Figure 3b shows the QE estimate, 1 - R, as a function of wavelength derived from these measurements. One can see a considerably better performance of the photodiode with the ARC, as expected. It also shows a calculated (1 - R) with ARC for the zero degree incidence angle, which can be directly compared to the QE estimated using the photocurrents. The maximum difference of the two techniques in the wavelength range 500–800 nm is about 8%.

5 Sensitivity

The sensitivity of the sensor was studied using the Time Over Threshold (TOT) mode of Timepix. This mode allows measurement of the flux in the sensor, and can therefore be used to compare

different sensors. The TOT technique works reasonably well for large fluxes, but has considerable non-linearity near the threshold. The limitation of this method comes from the fact that different Timepix chips have different threshold offsets and different gains which are difficult to calibrate, so even the relative comparison is difficult. However, this approach can provide a direct comparison of the sensitivity for sensors produced by different processes.

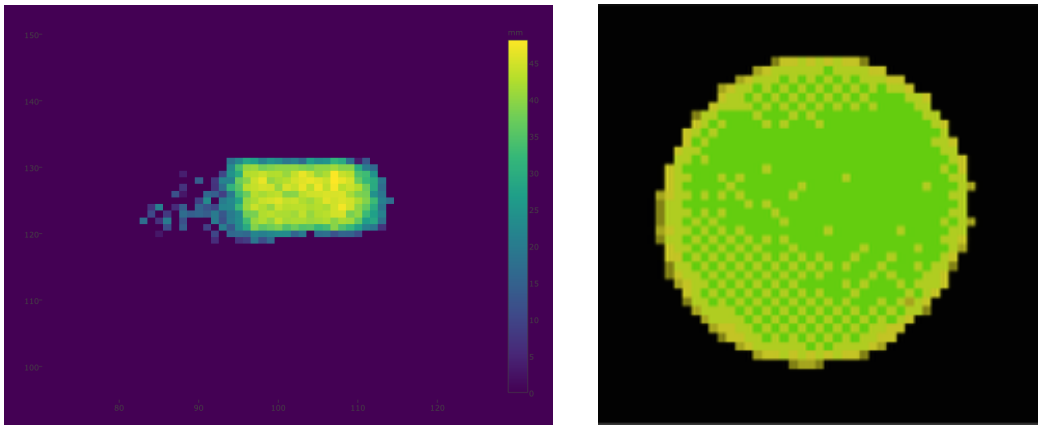

Figure 4. (a) Single TimepixCam frame with TOT signal induced by a 5V/50ns pulse applied to the LED, and b) an illustration of the "chessboard effect", see the text.

For this measurement, the sensor was illuminated with a LED. A pulse generator, Tektronix AFG3102C, provided synchronous pulses for the TimepixCam shutter and for the LED. The duration of the LED pulse was 50 nsec, with the light intensity controlled by the voltage across the LED. The light arrived at the sensor through a rectangular slit, which provided a convenient way to focus the camera lens. Several LEDs of different colors were selected to study the wavelength dependence. The wavelength response was measured using a Hamamatsu micro-spectrometer, C12880MA with 15 nm resolution, and was typically a well behaved line for each type of LED used. A typical single frame recorded during a LED pulse is shown in figure 4a. The TOT signal was induced by a 5V/50ns pulse applied to the LED.

Two sensors with surface passivations of 50 nm and 300 nm, were selected for the study. The thresholds for both sensors were chosen in a similar manner, close to the Timepix noise floor, to make their responses as similar as possible. The TOT data was taken for different LED illuminations by varying the voltage on the LED. Figure 5a shows the data as a function of voltage for the shortest LED wavelength, 405 nm.

These measurements were performed for each LED, and the ratio of TOT signal for the two types of sensors was calculated. To estimate the uncertainty, the ratios were averaged over a range of LED voltages, from 3 to 10V. The result of the ratio measurement is shown in figure 5b as a function of wavelength using five LEDs of different color. The vertical error bars correspond to the RMS error of averaging, while the horizontal error bars reflect the width of the LED emission spectrum. The ratio monotonically increases by about 20% from blue to red, in qualitative agreement with the expectation that the sensor with the thinner window would be more sensitive to the blue light.

We also compared the same sensors with 50 nm and 300 nm passivation in experiments with real ions in the BNL Chemistry Department using the setup and data described in [8], and found that

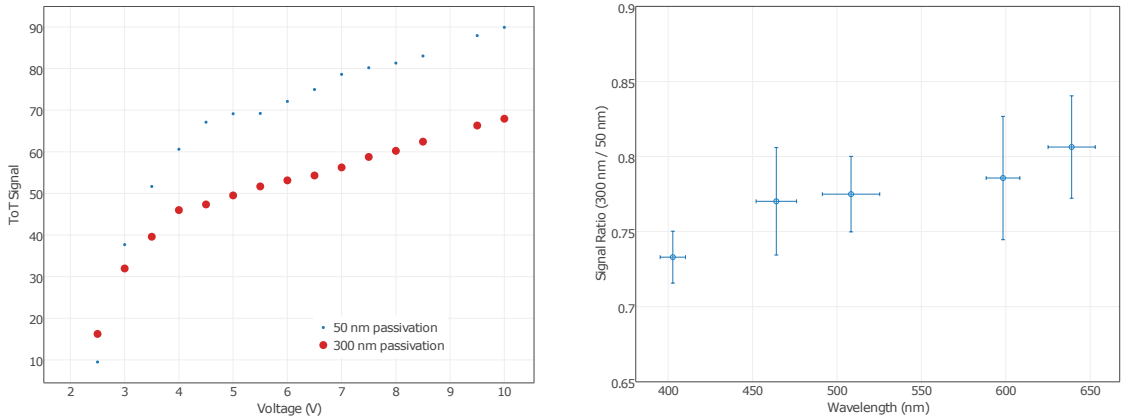

Figure 5. a) Measured TOT signal as a function of voltage for the LED with the shortest wavelength, 405nm, and b) the ratio of the TOT signal from the sensor with the 50 nm window thickness to the sensor with the 300 nm thickness as a function of wavelength.

the 50nm sensor was 3.1 times more efficient than the 300nm sensor for the equivalent experimental conditions in that particular setup. This is qualitatively consistent with the LED results above, and demonstrates that the thinnest sensor has considerably better performance. As mentioned in section 4, the quantitative comparison of these and the LED results above is complicated by the binary nature of the signal processing, which makes it dependent on the pixel thresholds.

For completeness, we note below another observation affecting measurements with Timepix-Cam, the so-called "chessboard effect" [12]. In Timepix, the neighboring pixels use complimentary clock phases to advance the counter, so one expects a variation of the measured time by one count in a chessboard arrangement across the chip. This variation affects the timing resolution and, in principle, could be corrected for. However, in practice, the correction is not possible, as a combination of several factors leads to a phase difference between the clock and the shutter which varies across the chip. This is caused by different delays during the buffering, and non-ideal 50/50 duty cycle of the clock.

Figure 4b shows a spot on the sensor illuminated with a fast laser, Picosecond Laser System EIG2000DX with a 443 nm head. One can clearly see the one count variation of the measured time in the bottom of the chip, its disappearance in the middle, and its reappearance on the top, shifted by one clock cycle. We also observed that this behavior is not stable, as the pattern can change from one laser shot to another for a fixed location on the chip.

6 Conclusion

We describe new results on the characterization of TimepixCam, an optical imager with 15ns time resolution. The quantum efficiency of the optimized sensor was measured to be better than 90% in the wavelength range from 430 to 900 nm using photodiodes produced in the same process. As expected, sensors with the smallest thickness of the entrance window, 50nm, were found to provide the best quantum efficiency and sensitivity to the blue light typically emitted by fast phosphors.

The current version of the camera can operate at a peak rate of 500 Hz, which can be sustained for two seconds. The maximum continuous rate of data taking is about 50 frames per second.

The Timepix ASIC itself supports the frame rate of a few kHz, and commercial readouts exist that enable this performance [13].

The produced sensors are also fully compatible with the new generation of time-stamping chips, Timepix3 [14]. Timepix3 has the same dimensions, while the timing resolution is improved by an order of magnitude to 1.5 ns. It also has multi-hit capability at the pixel level with only 0.5μs dead time. Preparation of a new camera with these sensors and Timepix3 readout is in progress.

Acknowledgments

The authors are grateful to Giulio Pellegrini and David Quirion from CNM for their help with the photodiodes; and to Victor Sanchez and Albert Sancho from X-Ray Imatek for their help with the XRI UNO camera. This work was supported by the BNL LDRD grant 13-006.

References

[1] D. Vu Truong Son et al., *Toward 100 mega-frames per second: design of an ultimate ultra-high-speed image sensor*, *Sensors* **10** (2009) 16.

[2] J. John et al., *PImMS, a fast event-triggered monolithic pixel detector with storage of multiple timestamps*, 2012 *JINST* **7** C08001.

[3] A. Nomerotski et al., *Pixel imaging mass spectrometry with fast and intelligent pixel detectors*, 20140 *JINST* **5** C07007.

[4] M. Brouard et al., *The application of the fast, multi-hit, pixel imaging mass spectrometry sensor to spatial imaging mass spectrometry*, *Rev. Sci. Instrum.* **83** (2012) 114101.

[5] J.H. Jungmann et al., *Fast, high resolution mass spectrometry imaging using a Medipix pixelated detector*, *J. Am. Soc. Mass Spectr.* **21** (2010) 2023.

[6] C. Vallance et al., *Fast sensors for time-of-flight imaging applications*, *Phys. Chem. Chem. Phys.* **16** (2014) 383.

[7] M.D. Kershis et al., *Exploring surface photoreaction dynamics using pixel imaging mass spectrometry (pimms)*, *J. Chem. Phys.* **139** (2013) 084202.

[8] M. Fisher-Levine and A. Nomerotski, *TimepixCam: a fast optical imager with time-stamping*, 2016 *JINST* **11** C03016.

[9] R. Ballabriga et al., *Review of hybrid pixel detector readout ASICs for spectroscopic X-ray imaging*, 2016 *JINST* **11** P01007.

[10] X. Llopart, R. Ballabriga, M. Campbell, L. Tlustos and W. Wong, *Timepix, a 65k programmable pixel readout chip for arrival time, energy and/or photon counting measurements*, *Nucl. Instr. Meth.* **A 581** (2007) 485.

[11] B. Winter, S. King, M. Brouard and C. Vallance, *A fast microchannel plate-scintillator detector for velocity map imaging and imaging mass spectrometry*, *Rev. Sci. Instrum.* **85** (2014) 023306.

[12] M. van Beuzekom, private communication.

[13] Amsterdam Scientific Instruments, Science Park 105, 1098 XG Amsterdam, Netherlands.

[14] T. Poikela et al., *Timepix3: a 65k channel hybrid pixel readout chip with simultaneous ToA/ToT and sparse readout*, 2014 *JINST* **9** C05013.